Human Molecular Genetics, 2003, Vol. 12, No. 9 **949–959**
DOI: 10.1093/hmg/ddg114

The *FMR1* CGG repeat mouse displays ubiquitin-positive intranuclear neuronal inclusions; implications for the cerebellar tremor/ataxia syndrome

Rob Willemsen[1,†], Marianne Hoogeveen-Westerveld[1,†], Surya Reis[1], Joan Holstege[2], Lies-Anne W.F.M. Severijnen[1], Ingeborg M. Nieuwenhuizen[1], Mariette Schrier[1], Leontine van Unen[1], Flora Tassone[3], Andre T. Hoogeveen[1], Paul J. Hagerman[3], Edwin J. Mientjes[1] and Ben A. Oostra[1,*]

[1]CBG-Department of Clinical Genetics and [2]Department of Neurosciences, Erasmus MC, Rotterdam, The Netherlands and [3]Department of Biological Chemistry, University of California, Davis, School of Medicine, Davis, CA, USA

Received November 1, 2002; Revised and Accepted February 24, 2003

Recent studies have reported that alleles in the premutation range in the *FMR1* gene in males result in increased *FMR1* mRNA levels and at the same time mildly reduced *FMR1* protein levels. Some elderly males with premutations exhibit an unique neurodegenerative syndrome characterized by progressive intention tremor and ataxia. We describe neurohistological, biochemical and molecular studies of the brains of mice with an expanded CGG repeat and report elevated *Fmr1* mRNA levels and intranuclear inclusions with ubiquitin, Hsp40 and the 20S catalytic core complex of the proteasome as constituents. An increase was observed of both the number and the size of the inclusions during the course of life, which correlates with the progressive character of the cerebellar tremor/ataxia syndrome in humans. The observations in expanded-repeat mice support a direct role of the *Fmr1* gene, by either CGG expansion *per se* or by mRNA level, in the formation of the inclusions and suggest a correlation between the presence of intranuclear inclusions in distinct regions of the brain and the clinical features in symptomatic premutation carriers. This mouse model will facilitate the possibilities to perform studies at the molecular level from onset of symptoms until the final stage of the disease.

INTRODUCTION

Fragile X syndrome, the most common inherited form of mental retardation, is almost exclusively caused by an expansion of a CGG repeat in the 5′ untranslated region of the *FMR1* gene. In the normal population, the CGG repeat is polymorphic and ranges from 5 to 50 CGGs with an average length of 30 CGG units (1). Fragile X patients have >200 CGG units (full mutation) that are usually hypermethylated and the methylation extends to the adjacent promoter region of *FMR1* (2–4). The gene is transcriptionally silenced and the gene product, the fragile X mental retardation protein (FMRP), is absent. The lack of FMRP in neurons is the cause of the mental retardation in fragile X patients (5,6). Unmethylated expansions of 50–200 CGG units, called premutations, are found in both males and females and may grow to a full mutation only upon maternal transmission to the next generation. The risk of transition is dependent on the size of the premutation and the smallest CGG repeat number known to expand to a full mutation is 59 repeats (7).

Individuals with a premutation were initially thought to have no phenotypic manifestations; however, a number of studies have reported mild learning disabilities and emotional problems in a small subgroup of premutation carriers (8). In addition, ∼20% of female premutation carriers manifest premature ovarian failure (POF) (9). Interestingly, recent studies have reported individuals with alleles in the premutation range

*To whom correspondence should be addressed at: CBG-Dept of Clinical Genetics, Erasmus MC, PO Box 1738, 3000 DR Rotterdam, The Netherlands. Tel: +31 104087198; Fax: +31 104089489; Email: b.oostra@erasmusmc.nl
†The authors wish it to be known that, in their opinion, the first two authors should be known as joint First Authors.

with increased *FMR1* mRNA levels that are up to 8-fold higher than normal and mildly reduced FMRP levels (10–12). Several studies have hypothesized that lengthened CGG repeats in the 5′ UTR lead to the translational impediment of the *FMR1* message and consequent FMRP reduction (10,12,13). The question whether these elevated *FMR1* mRNA levels and reduced FMRP levels result in a mild fragile X phenotype may need to be revisited by the recent description of older males carrying a premutation, who exhibit an unique neurodegenerative syndrome characterized by progressive intention tremor and ataxia. More advanced cases are accompanied by memory and executive function deficits, anxiety and eventual dementia (14,15). MRI studies (T_2 signal) of the brain of symptomatic adult male premutation carriers showed a characteristic imaging, including hyperintensities of the middle cerebellar peduncle, cerebellar white matter lateral, superior and inferior to the dentate nuclei and volume loss involving the pons, mesencephalon, cerebellar cortex, cerebral cortex, white matter of the cerebral hemispheres and corpus callosum (16). Neurohistological studies on the brains of four symptomatic elderly premutation carriers demonstrated neuronal degeneration in the cerebellum and the presence of eosinophilic intranuclear inclusions in both neurons and astroglia. Furthermore, the inclusions showed a positive reaction with anti-ubiquitin antibodies, which suggests a link with the proteasome degradation pathway (17). The origin and constitution of the inclusions is poorly understood; however, elevated *FMR1* mRNA levels have been proposed to be important for the formation of the inclusions (15).

To better understand the timing and mechanism involved in *FMR1* CGG repeat instability and methylation, we originally generated a mouse model in which the endogenous mouse CGG repeat was replaced by a human CGG repeat carrying 98 CGG units, which is in the premutation range (18). The 'knock-in' CGG triplet mouse shows moderate CGG repeat instability upon both maternal and paternal transmission. The recent clinical and molecular findings that premutation alleles may contribute to a specific tremor/ataxia syndrome in older males prompted us to further analyse the aging 'knock-in' CGG triplet mouse. Here we describe neurohistological, biochemical and molecular studies of the brains of these mice and report elevated *Fmr1* mRNA levels and intranuclear inclusions with ubiquitin, Hsp40 and the 20S catalytic core complex of the proteasome as constituents.

RESULTS

Quantification of *Fmr1* mRNA and *Fmrp*

We have analysed the expression of the *Fmr1* gene at the RNA and protein level in the expanded-repeat mice. The transcriptional activity of the *Fmr1* gene was determined by quantitative measurement of *Fmr1* mRNA levels using the fluorescence-based RT–PCR approach. The basis of this method is the accurate determination in the increase in *Fmr1*-specific amplicon during the early cycles of the PCR reaction. The level of *Fmr1* mRNA in expanded-repeat mice compared with control mice is determined using the expression of GUS mRNA in both mice as an internal control as is described by Tassone *et al.* (10). Figure 1 illustrates the relative *Fmr1* mRNA levels in brain tissue for the CGG expanded-repeat mice at different ages (1–72 weeks). It is evident from the data in Figure 1 that the *Fmr1* transcript levels were elevated and displayed ratios increased 2–3.5-fold relative to wild-type (wt) brain tissue. We have plotted only the data from the mice that were also used for immunohistochemistry; however, more mice at ages intermediate to the ones above were used for the quantification of *Fmr1* mRNA levels, and displayed elevated levels. In addition, for each individual mouse the exact length of the CGG repeat in tail DNA was determined (Fig. 1).

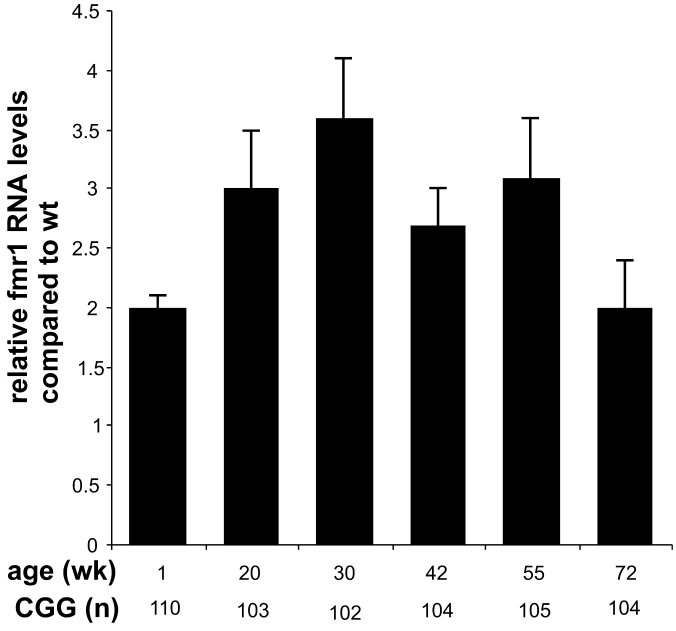

Figure 1. Relative *Fmr1* RNA levels by real-time fluorescent RT–PCR of brain of expanded-repeat mice compared with wild-type brain at age 1–72 weeks. The repeat length is determined of tail DNA at 10 days by the fragile X size polymorphism assay.

The level of FMRP is thought to be within the normal range in males with a premutation (6), although in premutation carriers with a higher number of repeats a decrease in FMRP levels has been described (10,12). To examine in mice the relationship between increased *Fmr1* mRNA levels and Fmrp levels we determined Fmrp levels in brain homogenates from expanded-repeat mice using quantitative immuno-precipitation (IP) and western blotting. If elevated *Fmr1* mRNA levels were positively correlated with Fmrp levels we would expect to see increased Fmrp levels. However, Figure 2 shows no obvious decrease in Fmrp levels in brain immunoprecipitates from a 72- and 30-week-old expanded-repeat mouse compared with wt mice (72 weeks old). No Fmrp was detected in the supernatants after IP (data not shown). Western blot analysis of total protein extracts with anti-actin antibodies shows that equivalent amounts of protein from the individual mice were used for the IP.

Immunohistochemistry and neuropathology

The brains of the different expanded-repeat mice were cut via the saggital suture and embedded in paraffin with the medial side downwards. Gross examination revealed no obvious

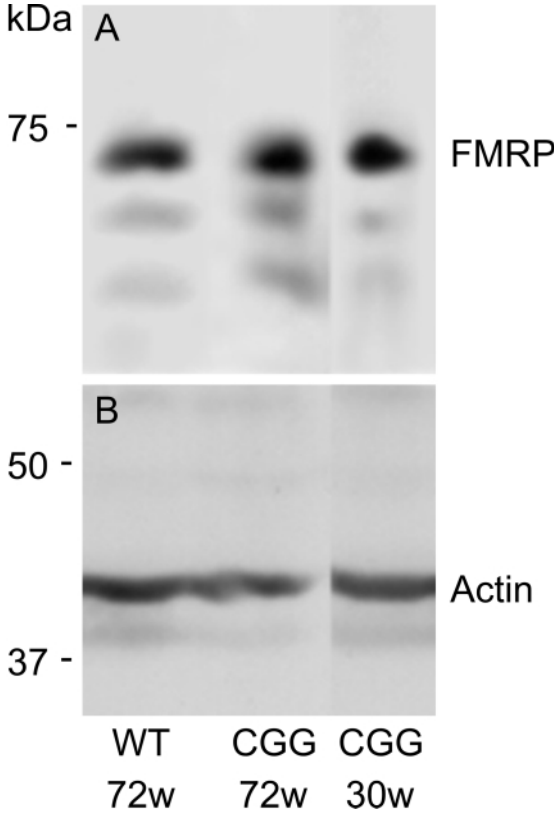

Figure 2. Western blot analysis of immunoprecipitated protein brain extracts from wild-type mice, 72 weeks (lane 1) and CGG expanded-repeat mice, 72 weeks (lane 2) and 30 weeks (lane 3). (**A**) immunoprecipitation with rabbit antibodies against FMRP followed by western blot analysis with monoclonal antibodies against FMRP. (**B**) Western blot analysis of total protein extracts with anti-actin antibody.

abnormalities compared with wild-type mice, including overall brain volume. Haematoxylin and eosin (H/E) stained saggital sections from the different expanded-repeat mice were examined for the presence of eosinophilic inclusions, as has been described for brain tissue of premutation males (17). Haematoxylin, a basic dye, binds to acidic components of a tissue (e.g. DNA and RNA) and gives a blue colour, while eosin, an acidic dye, binds to basic components of a tissue (e.g. cytoplasmic proteins) and gives a red colour. With this routine staining protocol we could not observe eosinophilic inclusions in the different expanded-repeat mice (20–72 weeks, data not shown). Further microscopic examination revealed no evident neuropathological phenomena, including neuronal cell loss, gliosis, astrocytosis (GFAP staining) and axonal torpedos. Since H/E staining revealed absence of inclusions we used as a next step to identify inclusions an immunocytochemical staining for ubiquitin, a hallmark for inclusions in neurons of affected premutation males. Three different antibodies directed against ubiquitin were used and all showed the presence of ubiquitin-positive inclusion bodies in neuronal nuclei. The results of monoclonal antibody FK1 is depicted in Figure 3A and B, illustrating the presence of poly-ubiquitinylated-positive inclusions in the nuclei of the parafascicular thalamic nucleus. The ubiquitin-positive inclusions could be observed only in nuclei of neurons throughout the brain, although very rarely a cytoplasmic inclusion could be observed (data not shown). Interestingly, each positively stained nucleus contained only a single inclusion. We have not observed nuclear inclusion in astrocytes, oligodendrocytes or microglial cells in any of the mice. Sections analysed from both wild-type and *Fmr1* knockout mice reveal a low level of cytoplasmic labelling with no evidence of intranuclear inclusions.

The average size of the inclusions within one specific brain region varied between the different expanded-repeat mice. In younger mice, smaller sized inclusions were present compared to older mice. Statistical analysis of the surface area of the inclusions in nuclei from the parafascicular thalamic nucleus between a 30 (mean 1.2 μm^2, SD 0.5) and 72-week-old (mean 3.5 μm^2, SD 1.0) expanded-repeat mouse revealed a highly significant difference ($P < 0.001$; *t*-test).

A comprehensive quantitative evaluation for the presence of ubiquitin-positive inclusions in the different paraffin embedded brain regions of five mice (20–72 weeks) is shown in Table 1. This systematic analysis demonstrates the presence of high percentages (>25%) of inclusions in specific brain structures, including olfactory nucleus, parafascicular thalamic nucleus, medial mammillary nucleus and colliculus inferior. Moderate percentages (10–25%) of inclusions were observed in the frontal cortex, pontine nucleus, vestibular nucleus and the tenth cerebellar lobule. In areas with high percentages of inclusions, the surface area of the inclusions tended to be larger compared with brain structures with low or moderate percentages of inclusions. Notably, it cannot be excluded that, due to our sampling and analysis method, some small brain areas with a relative high number of neurons with intranuclear inclusions have not been identified. We have used an alternative method to demonstrate the presence of ubiquitin-positive inclusions in brain tissue using frozen material instead of paraffin material. Cryostat sections from a 74-week-old expanded-repeat mouse showed similar results (data not shown).

Further research was focused on the constitution of the inclusions using an extensive panel of monoclonal and polyclonal antibodies directed against FMRP, proteins related to FMRP and proteins known to be involved in other disorders with inclusion formation (see Materials and Methods). Immunolabeling with antibodies against FMRP showed patterns of immunoreactivity seen in control animals, but failed to immunostain inclusions in brain areas known to contain high percentages of ubiquitin-positive intranuclear inclusions. An example is given in Figure 3C illustrating Fmrp distribution in the inferior colliculus (dorsal cortex) of a 72-week-old expanded-repeat mouse. As is described in Table 1, we find approximately half of the neurons with intranuclear inclusions. All the nuclei of the inferior colliculus (Fig. 3C) and other brain regions were totally devoid of Fmrp-positive inclusions. Fmrp distribution and quantity in the cell body of neurons of the expanded-repeat mouse appeared similar to wild-type mouse (compare Figure 3C and D), with the caveat that immunocytochemical analysis only allows semi-quantitative assessments. This similarity in quantity is in line with the data for Fmrp levels shown in Figure 2.

Immunolabelling of brain sections from a 72-week-old expanded-repeat mouse with other antibodies of the panel showed the presence of both Hsp40 (data not shown) and the

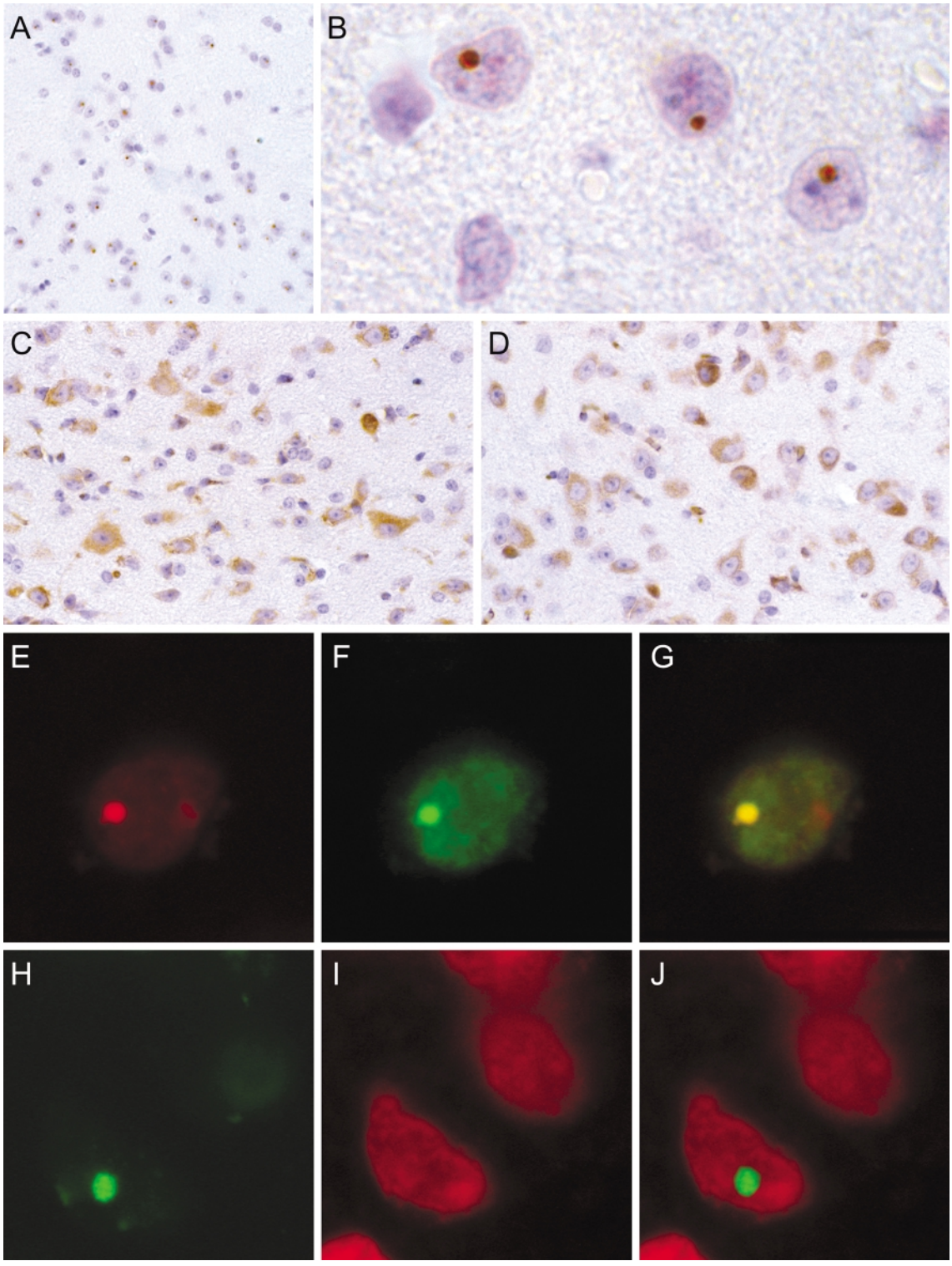

Figure 3. Immunohistochemical localization of ubiquitin in the parafascicular thalamic nucleus from the expanded-repeat mouse at the age of 72 weeks by an indirect immunoperoxidase technique (**A** and **B**). Note the presence of intranuclear ubiquitin-positive inclusions in approximately half of the nuclei at low magnification (A). The neurons in the inferior colliculus of both the expanded-repeat mouse (**C**; 72 weeks) and wild-type mouse (**D**) show almost similar levels of FMRP expression using monoclonal antibodies against FMRP. Colocalization of ubiquitin (**E**) and 20S proteasome (**F**) is shown in a neuron from the frontal cortex of the expanded-repeat mouse (72 weeks) using double-labelling immunofluorescence. Merge of the two signals demonstrates a clear colocalization of ubiquitin and the 20S proteasome within the intranuclear inclusions (**G**). Colocalization of ubiquitin (**H**) and ethidiumbromide staining for total RNA (**I**) in a neuron from the parafascicular thalamic nucleus of the expanded-repeat mouse (72 weeks) using immunofluorescence. Overlay of the two signals demonstrates that ethidium-bromide staining does not localize to ubiquitin-positive intranuclear inclusions (**J**). Magnifications: (A) 50×; (B) 400×; (C and D) 150×; (E–J) 700×.

Table 1. Quantitative analysis of ubiquitin-positive intranuclear inclusions in various brain structures

Brain structures	72 weeks		55 weeks		42 weeks		30 weeks		20 weeks	
	Nuclei	%	Nuclei	%	Nuclei	%	Nuclei	%	Nuclei	%
Frontal cortex	630/76	12	808/13	2	857/5	<1	1232/1	<1	1012/0	<1
Sensory/motor cortex	1671/52	3	1556/13	1	2025/0	<1	2454/0	<1	1976/0	<1
Cingulate cortex	602/54	9	740/15	2	816/2	<1	906/3	<1	859/0	<1
Visual cortex	508/5	1	953/4	<1	1279/0	<1	1099/1	<1	1190/0	<1
Hippocampus	1315/11	1	1446/5	<1	1056/0	<1	1642/0	<1	858/0	<1
Dentate gyrus	606/0	<1	1199/0	<1	2100/0	<1	1545/0	<1	859/0	<1
Hypothalamus (medial mammillary nucleus)	237/59	25	634/137	22	901/111	12	458/8	2	825/0	<1
Olfactory nucleus (anterior)	622/161	26	1629/108	7	596/28	5	1344/18	1	1092/1	<1
Striatum	506/4	1	1449/5	<1	1505/1	<1	1447/0	<1	929/0	<1
Substantia nigra	357/13	4	615/4	1	1380/2	<1	1184/3	<1	1006/0	<1
Parafascicular thalamic nucleus	1230/524	43	902/107	12	1634/217	13	1290/110	9	1005/0	<1
Colliculus inferior (dorsal cortex)	718/398	55	1184/226	19	1196/115	10	1022/40	4	875/7	1
Colliculus superior	1266/26	2	1395/8	1	1788/5	<1	1272/1	<1	1202/1	<1
Pontine nucleus	414/71	17	604/55	9	720/17	2	872/14	2	988/0	<1
Vestibular nucleus	503/74	15	547/44	8	534/16	3	639/10	2	986/0	<1
Purkinje cell layer	818/1	<1	573/0	<1	ND	—	393/0	<1	409/0	<1
Third cerebellar lobule (granular layer)	826/5	1	2188/6	<1	955/0	<1	1843/0	<1	1474/0	<1
Tenth cerebellar lobule (granular layer)	1185/256	22	3314/300	9	ND	—	1046/55	5	886/0	<1
Spinal cord (superficial dorsal horn)	1220/285	23	ND	—	ND	—	ND	—	ND	—
Spinal cord (deep dorsal horn)	1475/81	5	ND	—	ND	—	ND	—	ND	—
Spinal cord (ventral horn)	1137/33	3	ND	—	ND	—	ND	—	ND	—

20S catalytic core complex of the proteasome within a significant number of inclusions (Fig. 3E–G). Simultaneous labelling of ubiquitin (Fig. 3E, red) and the 20S complex (Fig. 3F, green) in a neuron of the frontal cortex revealed a clear co-localization (Fig. 3G, merge). We have tested antibodies against a number of proteins related to FMRP and proteins known to be involved in other disorders involving inclusion bodies: FXR1P, FXR2P, ribosomal P antigen, MAP2, tyrosine-tubulin, MAP1B, actin, SUMO-1, prion protein, neurofilament, GFAP, TAU, nucleolin, presinilin 1, α synuclein, Hsp70, Hsp60, Hsp27, Hsp72 and beta A4. All the antibodies displayed a specific labelling pattern in the brain, however, positive-labelled inclusions were not detected. In addition we tested the 1C2 antibody, which specifically recognizes pathogenic polyglutamine expansions in CAG expanded-repeat diseases (19). No specific labelling was seen in wild-type and expanded-repeat mice.

Microscopic visualization of DNA and total RNA was achieved by DAPI and ethidiumbromide staining, respectively. To study whether *Fmr1* transcripts or other RNA/DNA constituents were present within the inclusions a double labelling has been performed with ethidiumbromide (total RNA) staining (Fig. 3I, red) followed by immunoincubation with antibodies against ubiquitin (Fig. 3H, green). No co-localization could be observed (Fig. 3J, merge). A similar experiment using DAPI (DNA) staining after immunoincubation with antibodies against ubiquitin also showed no co-localization (data not shown), although due to the non-specific nature of this test, we cannot rule out a small accumulation of RNA within the inclusions.

A dramatic age-dependent somatic instability was reported in a transgenic mouse model for DM1 (20). We asked whether somatic instability coincides with the occurrence of inclusion bodies in the neurons. For each individual mouse the exact length of the CGG repeat was determined in tail DNA 10 days after birth (Fig. 1). We have observed somatic instability, but the increase in repeat length was never more than 10 repeats. An example is shown in Figure 4. The original repeat length of 102 CGGs in tail DNA at 10 days of age increased in week 52 to 104 CGGs in brain. The repeat was more unstable in kidney and testis with a mosaic pattern between 102 and 109 CGGs at 52 weeks of age.

DISCUSSION

Molecular findings

The mechanisms of CGG repeat instability is still poorly understood and attempts to generate transgenic mouse models with unstable CGG repeats were successful only very recently (18,21). Unfortunately, the inheritance of the CGG repeat is only moderately unstable, indicating differences between the behaviour of the *Fmr1* premutation CGG expanded-repeat in mouse and in human transmissions. Nevertheless, our data using a transgenic CGG expanded-repeat mouse model shows, as in humans, 2–3.5-fold elevated *Fmr1* mRNA levels in brain tissue compared with control. These elevated *Fmr1* message levels were already present in brain homogenates of pups at the age of 1 week. The increased *FMR1* message levels in cells from males carrying a premutation are intriguing and several mechanisms have been proposed. Tassone *et al.* (10) suggest that the elevated *FMR1* mRNA levels are due to increased transcriptional activity as compensatory mechanism for the diminished translational efficiency of the *FMR1* message, because no significant increase in *FMR1* mRNA stability was observed. In this hypothetical model the expanded CGG tract in the 5′-UTR of the message diminishes translation by a currently unknown mechanism. Conformational changes in the mRNA that influence the initiation of translation and stalled

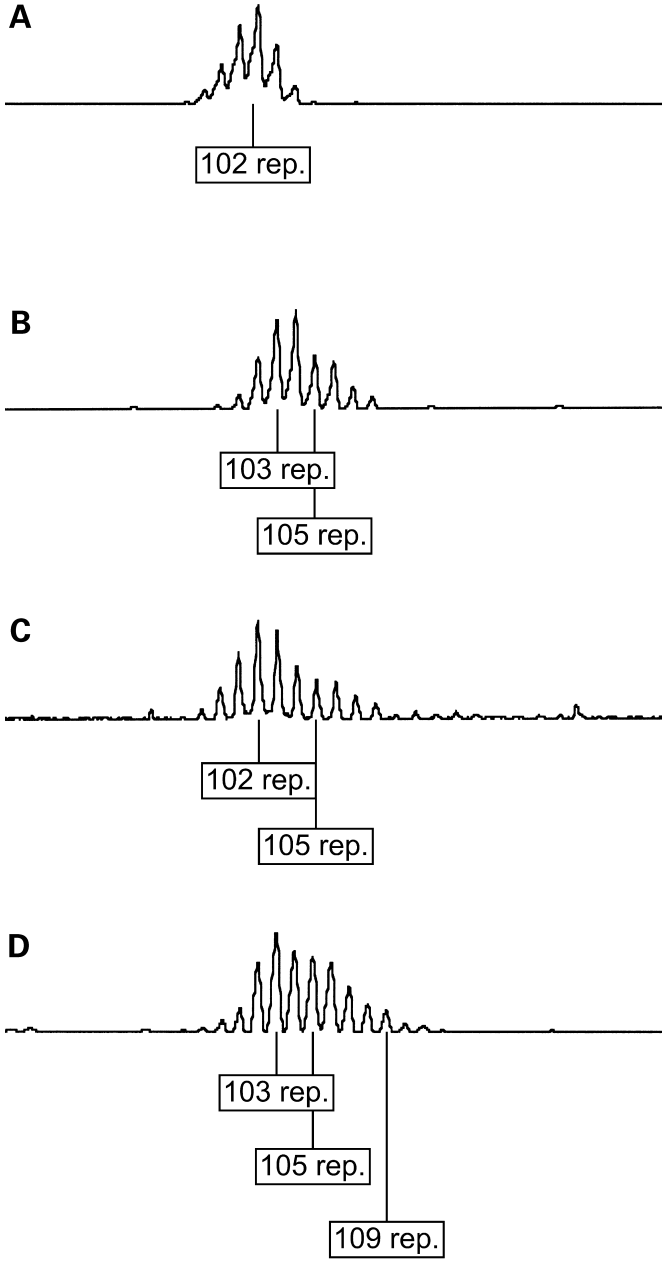

Figure 4. Somatic mutation analysis by fragile X size polymorphism assay. (**A**) Repeat length of tail DNA of an expanded-repeat male mouse was assayed at 10 days. The length in different tissues was determined again after 52 weeks: (**B**) brain; (**C**) kidney; (**D**) testis.

40S ribosomal subunits are proposed explanations (10,12,13,22). In addition, the expanded CGG repeat may lead to proportionally more open promoter conformation and consequently enhanced transcriptional activity (12). The normal *FMR1* message levels in the mutant I304N cell line argues against a role for the lack of functional FMRP as modulator of transcriptional activity of the *FMR1* gene (12,22). Another candidate for the up-regulation of the Fmr1 expression might be CGGBP1, a CGG binding protein, that has shown to be able to regulate expression from the FMR1 gene with a small CGG repeat (23). It can be hypothesized that in the case of an elongated CGG repeat the CGGBP1 might be sequestered due to extensive binding to the elongated repeat in the mRNA resulting in a lowered active concentration of CGGBP1. A lower CGGBP1 concentration results in an increased *FMR1* transcription.

Despite the elevated *Fmr1* message in brain tissue of expanded-repeat mice quantitative immunoprecipitation and western blotting showed comparable Fmrp levels. In contrast, cells from males carrying a premutation with elevated levels of *FMR1* message were accompanied by 20% reduced levels of FMRP in humans with a repeat of 100 CGGs (10,12,24). In the mouse the reduction in FMRP expression may be more subtle and below the detection level by the assay, or may differ between peripheral blood and brain.

For a number of trinucleotide repeat diseases the repeats are found to be somatically unstable, often varying from tissue to tissue. It is hypothesized that somatic mosaicism has some influence on the tissue specificity and the progression of the symptoms. Also in a number of mouse models, somatic instability has been seen (25–27) with dramatic instability seen in mouse models for HD and DM1 (20,28). The highest somatic instability in the DM1 model was an increase of over 500 repeats. We have tested the somatic instability in the CGG expanded-repeat mouse. Somatic instability was detected, although the increase was relatively small (less than 10 units). From this we conclude that somatic instability in the brain is not a general phenomenon but it cannot be excluded that it might play a role in the development of inclusion bodies in individual neurons.

Immuno-neuropathology

The present immunohistochemical study provides significant evidence for the presence of ubiquitin-positive intranuclear inclusions in neurons of the CGG expanded-repeat mouse. Ubiquitin-positive inclusions associated with CGG repeat expansions have recently been described in brains of males carrying a premutation (17). The authors reported the presence of eosinophilic ubiquitin-positive inclusions in both neuronal and astrocytic nuclei throughout the cerebrum and brainstem, but most prominent in the hippocampal formation. The inability to stain the mouse inclusions with eosin and the increase in size of the inclusions in time may reflect a progressive change of the composition of the inclusions. For the human brain, neuropathology was studied using post-mortem material; thus, examination was performed at the final stage of the tremor/ataxia syndrome with pronounced clinical features. In our expanded-repeat mice neuropathology was studied between 20 and 72 weeks before pronounced clinical features were obvious, however, extensive analysis of the phenotype of the expanded-repeat mice is necessary to determine both the onset and the development of the tremor/ataxia syndrome in mice. This study is in progress and will be addressed by combined MRI imaging and extensive behaviour studies. Perhaps older expanded-repeat mice (>72 weeks) will accumulate more aggregation-prone proteins within the inclusions and stain positive for eosin too. Another striking difference from humans is the absence in the mouse of astrocytic intranuclear inclusions and other neuropathologic

features, including neuronal loss, gliosis and marked dropout of Purkinje cells. Although the importance of astrocytic inclusions in man is still not understood, the absence of both astrocytic inclusions and the aforementioned neuropathology in the expanded-repeat mouse may reflect differences between species, like the eosin staining an early onset of the disease.

The origin of the intranuclear inclusions is unknown, however some characteristics are shared with hereditary ataxias linked to expansion of CAG repeats. Each of the polyglutamine diseases is characterized by neuronal intranuclear inclusions that consist of accumulations of insoluble aggregated polyglutamine-containing fragments (29). Unlike the hereditary ataxias, the *FMR1* premutation allele gives rise to the production of normal FMRP because the CGG expansion resides in the 5′ UTR of the *FMR1* mRNA. This would argue against the presence of Fmrp in the inclusions, as was demonstrated in the present study, however we cannot exclude the possibility that very small quantities of Fmrp, below the detection level of the immunocytochemical assay, are present in the inclusions. Alternatively, Fmrp although present, may be inaccessible in the protein aggregates. Further sophisticated analysis using mass spectrometry is in progress to address this issue.

The association of elevated *FMR1* message levels in connection with the tremor/ataxia syndrome raises the probability of the presence of *FMR1* transcripts within the inclusions. We have addressed this issue using double-labelling techniques in which ubiquitin was stained together with either ethidiumbromide or DAPI for detection of total RNA and DNA molecules, respectively (30). The lack of both total RNA and DNA indicates that they are not major constituents of the inclusions. The use of riboprobes to pick out single mRNA molecules are in progress, however to date the results are inconclusive.

The presence of both ubiquitin and the 20S core complex of the proteasome within the inclusions is intriguing and suggests a role of the proteasome degradation pathway in the cause of the cerebellar tremor/ataxia syndrome. In addition, the presence of Hsp40 (DnaJ family), a molecular chaperone that promotes cellular protein folding by binding unfolded polypeptides, within the inclusions indeed suggests involvement of the proteasome degradation pathway (31). Again, the presence of components of the ubiquitin–proteasome pathway is shared with several hereditary ataxias and other trinucleotide repeat disorders, including Huntington's disease (32,33), SCA type 1 (34), SCA type 3 (35), SCA type 7 (36) and OPMD (37). Whether the formation of aggregates underlies the clinical symptoms remains unsolved, and a direct toxic role for aggregates has been questioned. A model has been proposed in which the polyglutamine expansion has a toxic gain-of-function property on the protein, however a direct cause-and-effect relation between nuclear inclusions and the disease mechanisms is still under debate (29,38,39). Recent studies of cellular models of polyglutamine diseases point to impaired proteasome function in the presence of polyglutamine fragments. The cellular consequences of perturbation of the ubiquitin–proteasome degradation pathway in polyglutamine disorders may include transcriptional dysregulation of important genes, potentially leading to neuronal cell death (40,41). The model that aggregation-prone proteins can impede proteasome activity mediating neuronal dysfunction and death has also been proposed as a general model for a variety of the neurodegenerative diseases (29). The constitution of the inclusions in post-mortem brain tissue from males carrying a premutation is now under study, however, in the present study we have demonstrated that *Fmr1* mRNA and Fmrp are not the major constituents of the inclusions in mouse. The challenge for the near future is to identify the aggregation-prone proteins and/or mRNAs within the inclusions. One group of candidate proteins may include putative CGG binding proteins trapped by the expanded CGG *Fmr1* transcripts (23,42). Perhaps the long CGG tract in the mRNA attracts high quantities of CGG binding proteins with a consequent cumulative cytotoxic effect that may lead to intranuclear inclusion formation. Such a mechanism has been described for myotonic dystrophy (DM), where the expanded CTG repeat containing message is present in small intranuclear foci, and contributes to the constellation of features that characterize DM (43). In addition, the mutant RNA attracts high quantities of CUG binding proteins, which regulate alternative splicing of the insulin receptor and results in insulin resistance in myotonic dystrophy (44).

Clinical correlates

The presence of ubiquitin-positive intranuclear inclusions in neurons of all CGG mice at different ages (20–74 weeks) provides evidence for a common neuropathological hallmark associated with *Fmr1* premutation alleles. The increase of both the number and the size of the inclusions during the course of life correlate with the progressive character of the cerebellar tremor/ataxia syndrome in humans and suggest that inclusion formation plays a critical role in the onset and development of the syndrome.

The main and first presenting symptoms observed in the group of symptomatic premutation carriers is a progressive intention tremor and a gait ataxia with loss of balance and a tendency to fall. These motor disturbances are usually ascribed to cerebellar dysfunction. However, as in humans, intranuclear inclusions were absent in Purkinje cells and very limited in the granular layer, with the exception of lobule 10 in the posterior cerebellum of the mouse, which showed relatively high numbers of granule cells with intranuclear inclusions. The affected part of the cerebellum is also known as the vestibulo-cerebellum, because of its direct connections with the vestibular nuclei, which also showed relatively high numbers of neurons with intranuclear inclusions. Therefore it seems likely that patients with the cerebellar symptoms like ataxia with imbalance and the tendency to fall are due for a major part to dysfunction of the vestibulo-cerebellum and the vestibular system. Problems with eye movements as suggested by the mild saccadic pursuit that was found in some patients (14) also point to involvement of the vestibular nuclei.

Other cerebellar symptoms in the patients, especially the intention tremor, are usually attributed to the cerebro-cerebellum, the largest part of the cerebellum, receiving input from cortical motor areas by way of the pontine nuclei. In our mice nuclear inclusions were very low in the cerebro-cerebellum and also appeared low in the cerebellar nuclei (data not shown). However, the pontine nuclei did show a relatively high number of cells with intranuclear inclusions as also described in humans (17). Furthermore, in MRI studies of

the patients, a decrease was found in size of the pons and the medial cerebellar peduncle, which contains the axons projecting from the pontine nuclei to the cerebellar cortex (16). Dysfunction of the pontine nuclei may thus contribute to disturbed granule cell input and impaired cerebellar functioning. It should be noted that, unlike the mouse, there is substantial Purkinje cell dropout in the cerebellums of the affected human carriers; that neuropathologic change is likely to play a prominent role in the clinical findings in humans.

Some of the motor deficits in the patients, like resting tremor and rigidity, are usually regarded as Parkinson's disease-like symptoms and thus attributed to lowered levels of dopamine in the striatum due to degeneration of dopaminergic cells in the substantia nigra. However, neither the substantia nigra nor the striatum showed any nuclear inclusions in our expanded-repeat mice and were relatively limited in humans (17). Interestingly, in our expanded-repeat mice we found intranuclear inclusions in a relatively high number of cells in the posterior part of the thalamus, which we identified as the parafascicular thalamic nucleus. This thalamic nucleus has strong connections with the striatum, rather than with cortical areas as most parts of the thalamus (45). It has further been suggested that a decrease in activity in the parafascicular nucleus leads to a decrease in dopamine release in the striatum (46). Thus the mild Parkinson's disease-like symptoms in the patients may be explained by dysfunction of the parafascicular thalamic nucleus.

With respect to motor functioning it should be added that the patients lack any signs of muscle weakness or other signs of higher or lower motoneuron disease. This fits well with the absence of intranuclear inclusions in motoneuronal nuclei (although some intranuclear inclusions were observed in the neuropil of the ventral horn) and the relatively low number of intranuclear inclusions in the (primary) motor areas. A general survey of the main cortical areas shows that inclusions occur, especially in the frontal cortex and in the cingulate cortex, whereas more posterior parietal and visual areas were much less affected. These findings are in agreement with findings in the brain of human adult fragile X premutation carriers, although in their analysis inclusions were present more or less equally throughout the cortex (17). Our finding that inclusions are preferentially located in the frontal and cingulate cortex would fit with findings that symptomatic adult fragile X premutation carriers show cognitive and emotional decline. Memory loss has also been described in these patients and fits with pathological findings in human patients who show many affected neurons in the hippocampus. Surprisingly, in the present study, no pathology was found in the hippocampus or the dentate gyrus. However, we did find relatively high numbers of neurons with intranuclear inclusions in the mammillary bodies. These nuclei, which are part of the hypothalamus, are strongly involved in memory formation, especially of recent events both in human (47) and in rat (48). Whether our mice show memory deficits in behavioural tests is presently being investigated.

A surprising finding was that the inferior colliculus showed the highest percentage of cells with nuclear inclusions. Since all auditory pathways from the cochlea converge onto the inferior colliculus, impairment of inferior collicular functioning would lead to hearing problems (49). Interestingly, two of the five patients described by Hagerman *et al.* (14) had bilateral hearing loss at a relatively early age, suggesting that decreased functioning of the inferior colliculus occurred in these patients.

In conclusion, the observations in expanded-repeat mice suggest a correlation between the presence of intranuclear inclusions in distinct regions of the brain and the clinical features in symptomatic premutation carriers. Moreover, the presence of inclusions in expanded-repeat mice supports a direct role of the *Fmr1* gene, by either CGG expansion *per se* or mRNA level, in the formation of the inclusions, which in humans could also be explained by a synergistic effect with another genetic locus. The presence of ubiquitin, 20S proteasome complex and molecular chaperone Hsp40 within the intranuclear inclusions strongly indicates perturbation of normal proteasome degradation pathways in the CGG expanded-repeat mouse. Thus, inclusion formation seems to play a crucial role in the development of the tremor/ataxia syndrome among older males carrying a premutation. The challenge for the near future is to understand the origin of the inclusions, their constitution and how dysfunction of the proteasome is related to the syndrome. Although the frequency of the tremor/ataxia syndrome among carriers remains to be established it is now apparent that premutation alleles contribute to a phenotype at later age. This might be important for premutation carriers (1:800) (50) with a repeat size >71 CGG repeats, who have until recently been thought to be without a clinical phenotype since Greco *et al.* (17) described a case with a premutation of 71 CGG repeats in which inclusion bodies have been found. This mouse model will facilitate the possibilities to perform studies at the molecular level from onset of symptoms until the final stage of the disease. Ultimately, this mouse model might contribute to knowledge and understanding of how neurons die in a variety of neurodegenerative diseases, including Alzheimer's disease, Parkinson's disease, amyotrophic lateral sclerosis, tauopathies and polyglutamine diseases.

MATERIALS AND METHODS

Tissues and antibodies

Mice carrying a human (CGG) repeat (from 102 to 110 units), varying in age from 1 to 74 weeks old, were sacrificed, and brain tissue was isolated and cut sagittally into two equal pieces. One part was immediately frozen in liquid nitrogen for RNA extraction, and quantitative western blotting. The other part was immediately fixed in 4% paraformaldehyde for immunohistochemistry.

The following monoclonal and polyclonal antibodies were used: rabbit anti-ubiquitin (1:500, DAKO), mouse anti-ubiquitin (FK1, 1:100 recognize only poly-ubiquitinylated proteins; FK2, 1:100 recognize both poly- and mono-ubiquitinylated proteins, both from Affiniti), rabbit anti-FMRP (51), mouse anti-FXR1P (52), rabbit anti-FXR2P (53), human anti-ribosomal P antigen (PO, 1:100, Immunovision), mouse anti-MAP2 (1:100, Boehringer), mouse anti-tyrosine-tubulin (1:100, Sigma), mouse anti-MAP1B (1:100, Sigma), mouse anti-actin (1:100, Sigma), rabbit anti-SUMO-1 (FL-1-101, 1:100, Santa Cruz), goat anti-prion protein ($PrP_{27–30}$, 1:500, Chemicon), mouse anti-neurofilament (SMI-32, 1:1000,

Sternberger monoclonals), mouse anti-GFAP (1:500, DAKO), mouse anti-TAU (BR01, 1:500, Innogenetics), mouse anti-nucleolin (C23, 1:100, Santa Cruz), mouse anti-polyglutamine (1C2, 1:1000, Chemicon), rabbit anti-20S core complex of the proteasome (54), goat anti-presinilin 1 (C20, 1:100, Sanvertech), rabbit anti-α synuclein (1:100, Chemicon), rabbit anti-Hsp70 (1:100, Sanvertech), rabbit anti-Hsp25 (1:100, Sanvertech), goat anti-Hsp27 (1:100, Sanvertech), rabbit anti-Hsp40 (1:100, Stressgen), rabbit anti-Hsp60 (1:100, Stressgen), and mouse anti-Hsp72 (1:100, Amersham), and mouse anti-beta A4 (1:100 +90% formic acid, DAKO).

Visualization of the primary antibodies was performed with rabbit anti-mouse (Ig)/HRP (1:100, DAKO), swine anti-rabbit (Ig)/HRP (1:100, DAKO), rabbit anti-goat (Ig)/HRP (1:100, DAKO), goat anti-human (Ig)/HRP (1:100, DAKO), goat anti-mouse (Ig)/FITC (1:100, Sigma) or goat anti-rabbit/TRITC (1:100, DAKO).

RNA-isolation and RT–PCR analysis

Brains were homogenized under liquid nitrogen and divided into two parts for RNA and protein isolation. Total RNA was isolated from brain by extraction with the single-step acid phenol method, using RNAzol B (Tel-Test Inc.) and employed for quantitative fluorescent RT–PCR. Total RNA was treated with RQ DNase I (Promega) for 30 min at 37°C followed by phenol extraction. The total RNA was analyzed spectrophotometrically for purity and quantity. The RNA was stored at −80°C until use.

One microgram of total RNA was pre-incubated with 0.6 μg random hexamers (Pharmacia) and oligo(dT)$_{12–18}$ (Pharmacia) at 65°C for 10 min. cDNA synthesis was then carried out at 42°C for 120 min in a total volume of 25 μl with 180 U SSII-RT and supplier's buffer (Invitrogen), 1 mM DTT, 10 U RNase inhibitor (Invitrogen), 0.8 mM each dNTP. For a quantitative estimate of the relative *Fmr1* mRNA levels, we adapted the technique described by Tassone *et al.* (10), using an ABI7700 Sequence Detector with Applied Biosystems SYBR Green PCR master mix (P/N 4309155). The*Fmr1* amplicon is a 134 bp product spanning the junction between exons 6 and 7 of the gene (positions 581–715 of GenBank sequence NM_008031). The following primers were used: forward, 5′-CAG TTG GTG CCT TTT CTG TAA CT-3′; reverse, 5′-GAG ACA ACT TAG TGC GCA GAC T-3′. The relativea bundance of *Fmr1* mRNA was assessed by comparison with the mouse β-gluronidase (GUS) mRNA (GenBank accession number NM_010368.1) for a 63 bp amplicon detected with primers: forward, 5′-CTG GAG GAT TGC CAA CGA A-3′ and; reverse 5′ GCT TCC GAA ACA CTG GGT TCT 3′. For each sample there was 1 μl of cDNA added to the master PCR mix and taken in triplicate and *Fmr1* and *GUS* reactions were run in parallel. The final reaction volume was 25 μl in the Applied Biosystems SYBR Green PCR master mix (P/N 4309155) with 5 or 10 μM of each primer. Cycle parameters were 2 min at 50°C and 10 min at 95°C, followed by 45 cycles with 15 s at 95°C denaturation and 1 min at 60°C annealing/extension. Relative *Fmr1* levels were calculated as follows: $2^{-[-\Delta C_t(\text{fragile X}) - \Delta C_t(\text{control})]} = 2^{-\Delta C_t}$, where ΔC_t equals $C_t(FMR1) - C_t(GUS)$ as discussed in Tassone *et al.* (10). At the end of each PCR run, a dissociation curve analysis was performed. In addition, gel electrophoresis was performed to confirm the correct size of the amplicon and the absence of non-specific bands. Each sample was assayed a minimum of two times.

DNA analysis

DNA was extracted from mouse tissue or tail by incubating with Protein K in 335 μl lysis buffer (10 mM Tris–HCl, 400 mM NaCl, 2 mM EDTA pH 7.3–7.4, 1% SDS) overnight at 55°C NaCl, 150 μl 6 M, was added and the suspension was centrifuged. To the supernatant two volumes 96% ethanol were added to precipitate the DNA. DNA was dissolved in 100 μl H_2O. The fragile X size polymorphism assay (Perkin Elmer Biosystems) was used to determine the exact length of the CGG repeat. PCR conditions were as described by the Perkin Elmer Biosystems. PCR samples were analysed with an ABI3100 sequencer (PE Biosystems).

Immunoprecipitation (IP) and western blotting

Equal amounts of extracts from mouse brains were incubated at room temperature for 1 h in a final volume of 0.5 ml of the protein extraction buffer [10 mM Hepes, 300 mM KCl, 5 mM $MgCl_2$, 5 mM $CaCl_2$, 0.45% Trition X-100, 0.05% Tween, pH 7.6; protease inhibitor cocktail mix (Roche), containing 50 μl protein-A-sepharose beads (Amersham)]. The pre-cleared supernatants were incubated overnight at 4°C with antibody KI, a rabbit polyclonal antibody directed against the C-terminal part of FMRP, followed by an incubation for 2 h at room temperature with 50 μl protein-A-sepharose beads. Subsequently, the beads were extensively washed with the extraction buffer. The immunoprecipitated proteins were electrophoresed on a 7.5% SDS–polyacrylamide gel. Ten percent of protein extracts used for the IP was applied for direct western blotting. Following SDS–PAGE, proteins were electroblotted onto a nitrocellulose membrane. Mouse antibodies against FMRP (51) and against α-actin (1:3000, Sigma) were used as primary antibodies for immunodetection. Horseradish peroxidase labelled anti-mouse IgG was used as secondary antibody, allowing chemiluminesce detection with ECL KIT (Amersham).

Immunohistochemistry

Brain tissues (20-, 30-, 42-, 55- and 72-week-old mice) were fixed overnight at 4°C and embedded sagittally in paraffin according to standard protocols. Sections (5 μm) were cut, deparaffinized and hydrated followed by microwave treatment and subsequent indirect immunoperoxidase labeling for the antibodies described above. Brain tissue of a 74-week-old mouse was embedded in Tissue Tek (Miles laboratory) and frozen in liquid nitrogen for cryostat sections. For a detailed protocol for both paraffin and cryostat sections see Bakker *et al.* (55). Routine histological analysis was performed on haematoxylin and eosin stained sections. For quantitative analysis of the number of ubiquitin-positive nuclear inclusions, each brain (20–72 weeks) was sectioned from medial to lateral direction and at 50 μm intervals each section was incubated with anti-ubiquitin antibodies for comprehensive analysis for the presence of ubiquitin

inclusions in the different brain regions. The brain of the 72-week-old mouse was used to identify the brain regions that showed high numbers of ubiquitin-positive intranuclear inclusions. In addition, we have included some regions of interest on the basis of the phenotype described in symptomatic premutation carriers (see Table 1). The different regions were recognized using the mouse brain atlas (56) and the number of inclusions was expressed as a percentage of the total number of nuclei examined in that particular brain region. For double immuno-fluorescence labelling (74-week-old mouse only), mouse anti-ubiquitin (FK1, Affiniti) was mixed with rabbit anti-20S proteasome in the first incubation step, followed by a secondary step with a mixture containing anti-rabbit conjugated with FITC and anti-mouse conjugated with TRITC. Visualization of DNA and total cellular RNA by ethidiumbromide or DAPI in combination with mouse anti-ubiquitin (FK1, Affiniti) incubation was performed by using the protocol according to Tang *et al.* (30). The surface area of the ubiquitin-positive inclusions were estimated by using the Leica Image Analysis system.

Brain sections from wild-type and *Fmr1* knockout mouse (both 72 weeks old) were used as a control for the presence and labeling specificity of both ubiquitin-positive nuclear inclusions and the expression level of Fmrp in neurons.

ACKNOWLEDGEMENTS

The authors wish to thank Tom de Vries Lentsch for excellent photography. Antibodies against rat 20S proteasome and FXR1P were kindly provided by Dr W. Ward and Dr B. Bardoni, respectively. Special thanks to Dr P. Rizzu for antibodies against Hsp40 and Hsp60 and stimulating discussions. M.S. was supported by Human Frontier Science Program grant RGP0052 and B.O. was supported by NIH 5R01 HD38038. This research was also supported by NIH R01 HD40661 (P.J.H.).

REFERENCES

1. Fu, Y.H., Kuhl, D.P., Pizzuti, A., Pieretti, M., Sutcliffe, J.S., Richards, S., Verkerk, A.J., Holden, J.J., Fenwick, R. Jr, Warren, S.T. *et al.* (1991) Variation of the CGG repeat at the fragile X site results in genetic instability: resolution of the Sherman paradox. *Cell*, **67**, 1047–1058.
2. Oberlé, I., Rousseau, F., Heitz, D., Kretz, C., Devys, D., Hanauer, A., Boue, J., Bertheas, M.F. and Mandel, J.L. (1991) Instability of a 550-base pair DNA segment and abnormal methylation in fragile X syndrome. *Science*, **252**, 1097–1102.
3. Verkerk, A.J., Pieretti, M., Sutcliffe, J.S., Fu, Y.H., Kuhl, D.P., Pizzuti, A., Reiner, O., Richards, S., Victoria, M.F., Zhang, F.P. *et al.* (1991) Identification of a gene (FMR-1) containing a CGG repeat coincident with a breakpoint cluster region exhibiting length variation in fragile X syndrome. *Cell*, **65**, 905–914.
4. Sutcliffe, J.S., Nelson, D.L., Zhang, F., Pieretti, M., Caskey, C.T., Saxe, D. and Warren, S.T. (1992) DNA methylation represses FMR-1 transcription in fragile X syndrome. *Hum. Mol. Genet.*, **1**, 397–400.
5. Pieretti, M., Zhang, F.P., Fu, Y.H., Warren, S.T., Oostra, B.A., Caskey, C.T. and Nelson, D.L. (1991) Absence of expression of the FMR-1 gene in fragile X syndrome. *Cell*, **66**, 817–822.
6. Verheij, C., Bakker, C.E., de Graaff, E., Keulemans, J., Willemsen, R., Verkerk, A.J., Galjaard, H., Reuser, A.J., Hoogeveen, A.T. and Oostra, B.A. (1993) Characterization and localization of the FMR-1 gene product associated with fragile X syndrome. *Nature*, **363**, 722–724.
7. Nolin, S.L., Lewis, F.A., Ye, L.L., Houck, G.E., Glicksman, A.E., Limprasert, P., Li, S.Y., Zhong, N., Ashley, A.E., Feingold, E. *et al.* (1996) Familial transmission of the FMR1 CGG repeat. *Am. J. Hum. Genet.*, **59**, 1252–1261.
8. Hagerman, R.J. (2002) The physical and behavioural phenotype. In Hagerman, R.J. and Hagerman, P. (eds), *Fragile-X Syndrome: Diagnosis, Treatment and Research.* The Johns Hopkins University Press, Baltimore, MD, pp. 3–109.
9. Sherman, S.L. (2000) Premature ovarian failure in the fragile X syndrome. *Am. J. Med. Genet.*, **97**, 189–194.
10. Tassone, F., Hagerman, R.J., Taylor, A.K., Gane, L.W., Godfrey, T.E. and Hagerman, P.J. (2000) Elevated levels of FMR1 mRNA in carrier males: a new mechanism of involvement in the Fragile-X syndrome. *Am. J. Hum. Genet.*, **66**, 6–15.
11. Tassone, F., Hagerman, R.J., Taylor, A.K., Mills, J.B., Harris, S.W., Gane, L.W. and Hagerman, P.J. (2000) Clinical involvement and protein expression in individuals with the FMR1 premutation. *Am. J. Med. Genet.*, **91**, 144–152.
12. Kenneson, A., Zhang, F., Hagedorn, C.H. and Warren, S.T. (2001) Reduced FMRP and increased FMR1 transcription is proportionally associated with CGG repeat number in intermediate-length and premutation carriers. *Hum. Mol. Genet.*, **10**, 1449–1454.
13. Feng, Y., Zhang, F.P., Lokey, L.K., Chastain, J.L., Lakkis, L., Eberhart, D. and Warren, S.T. (1995) Translational suppression by trinucleotide repeat expansion at FMR1. *Science*, **268**, 731–734.
14. Hagerman, R.J., Leehey, M., Heinrichs, W., Tassone, F., Wilson, R., Hills, J., Grigsby, J., Gage, B. and Hagerman, P.J. (2001) Intention tremor, parkinsonism, and generalized brain atrophy in male carriers of fragile X. *Neurology*, **57**, 127–130.
15. Hagerman, R.J. and Hagerman, P.J. (2002) The fragile X premutation: into the phenotypic fold. *Curr. Opin. Genet. Dev.*, **12**, 278–283.
16. Brunberg, J.A., Jacquemont, S., Hagerman, R.J., Berry-Kravis, E.M., Grigsby, J., Leehey, M.A., Tassone, F., Brown, W.T., Greco, C.M. and Hagerman, P.J. (2002) Fragile X premutation carriers: characteristic MR imaging findings of adult male patients with progressive cerebellar and cognitive dysfunction. *Am. J. Neuroradiol.*, **23**, 1757–1766.
17. Greco, C.M., Hagerman, R.J., Tassone, F., Chudley, A.E., Del Bigio, M.R., Jacquemont, S., Leehey, M. and Hagerman, P.J. (2002) Neuronal intranuclear inclusions in a new cerebellar tremor/ataxia syndrome among fragile X carriers. *Brain*, **125**, 1760–1771.
18. Bontekoe, C.J., Bakker, C.E., Nieuwenhuizen, I.M., van Der Linde, H., Lans, H., de Lange, D., Hirst, M.C. and Oostra, B.A. (2001) Instability of a (CGG)(98) repeat in the Fmr1 promoter. *Hum. Mol. Genet.*, **10**, 1693–1699.
19. Trottier, Y., Lutz, Y., Stevanin, G., Imbert, G., Devys, D., Cancel, G., Saudou, F., Weber, C., David, G., Tora, L. *et al.* (1995) Polyglutamine expansion as a pathological epitope in Huntington's disease and four dominant cerebellar ataxias. *Nature*, **378**, 403–405.
20. Fortune, M.T., Vassilopous, C., Coolbaugh, M.I., Siciliano, M.J. and Monckton, D.G. (2000) Dramatic, expansion-biased, age-dependent, tissue-specific somatic mosaicism in a transgenic mouse model of triplet repeat instability. *Hum. Mol. Genet.*, **9**, 439–445.
21. Peier, A. and Nelson, D. (2002) Instability of a premutation-sized CGG repeat in FMR1 YAC transgenic mice. *Genomics*, **80**, 423–432.
22. Tassone, F., Hagerman, R.J., Chamberlain, W.D. and Hagerman, P.J. (2000) Transcription of the FMR1 gene in individuals with fragile X syndrome. *Am. J. Med. Genet.*, **97**, 195–203.
23. Muller-Hartmann, H., Deissler, H., Naumann, F., Schmitz, B., Schroer, J. and Doerfler, W. (2000) The human 20-kDa 5′-(CGG)(n)-3′-binding protein is targeted to the nucleus and affects the activity of the FMR1 promoter. *J. Biol. Chem.*, **275**, 6447–6452.
24. Primerano, B., Tassone, F., Hagerman, R.J., Hagerman, P., Amaldi, F. and Bagni, C. (2002) Reduced FMR1 mRNA translation efficiency in Fragile X patients with premutations. *RNA*, **8**, 1–7.
25. Mangiarini, L., Sathasivam, K., Mahal, A., Mott, R., Seller, M. and Bates, G.P. (1997) Instability of highly expanded CAG repeats in mice transgenic for the Huntington's disease mutation. *Nat. Genet.*, **15**, 197–200.
26. Seznec, H., Lia-Baldini, A.S., Duros, C., Fouquet, C., Lacroix, C., Hofmann-Radvanyi, H., Junien, C. and Gourdon, G. (2000) Transgenic mice carrying large human genomic sequences with expanded CTG repeat mimic closely the CM CTG repeat intergenerational and somatic instability. *Hum. Mol. Genet.*, **9**, 1185–1194.

27. Ishiguro, H., Yamada, K., Sawada, H., Nishii, K., Ichino, N., Sawada, M., Kurosawa, Y., Matsushita, N., Kobayashi, K., Goto, J. *et al.* (2001) Age-dependent and tissue-specific CAG repeat instability occurs in mouse knock-in for a mutant Huntington's disease gene. *J. Neurosci. Res.*, **65**, 289–297.
28. Wheeler, V.C., Auerbach, W., White, J.K., Srinidhi, J., Auerbach, A., Ryan, A., Duyao, M.P., Vrbanac, V., Weaver, M., Gusella, J.F. *et al.* (1999) Length-dependent gametic CAG repeat instability in the Huntington's disease knock-in mouse. *Hum. Mol. Genet.*, **8**, 115–122.
29. Taylor, J.P., Hardy, J. and Fischbeck, K.H. (2002) Toxic proteins in neurodegenerative disease. *Science*, **296**, 1991–1995.
30. Tang, S.J., Meulemans, D., Vazquez, L., Colaco, N. and Schuman, E. (2001) A role for a rat homolog of staufen in the transport of RNA to neuronal dendrites. *Neuron*, **32**, 463–475.
31. Cummings, C.J., Mancini, M.A., Antalffy, B., DeFranco, D.B., Orr, H.T. and Zoghbi, H.Y. (1998) Chaperone suppression of aggregation and altered subcellular proteasome localization imply protein misfolding in SCA1. *Nat. Genet.*, **19**, 148–154.
32. Davies, S.W., Turmaine, M., Cozens, B.A., DiFiglia, M., Sharp, A.H., Ross, C.A., Scherzinger, E., Wanker, E.E., Mangiarini, L. and Bates, G.P. (1997) Formation of neuronal intranuclear inclusions underlies the neurological dysfunction in mice transgenic for the HD mutation. *Cell*, **90**, 537–548.
33. Petersen, A., Larsen, K.E., Behr, G.G., Romero, N., Przedborski, S., Brundin, P. and Sulzer, D. (2001) Expanded CAG repeats in exon 1 of the Huntington's disease gene stimulate dopamine-mediated striatal neuron autophagy and degeneration. *Hum. Mol. Genet.*, **10**, 1243–1254.
34. Koyano, S., Iwabuchi, K., Yagishita, S., Kuroiwa, Y. and Uchihara, T. (2002) Paradoxical absence of nuclear inclusion in cerebellar Purkinje cells of hereditary ataxias linked to CAG expansion. *J. Neurol. Neurosurg. Psychiat.*, **73**, 450–452.
35. Schmidt, T., Lindenberg, K.S., Krebs, A., Schols, L., Laccone, F., Herms, J., Rechsteiner, M., Riess, O. and Landwehrmeyer, G.B. (2002) Protein surveillance machinery in brains with spinocerebellar ataxia type 3: redistribution and differential recruitment of 26S proteasome subunits and chaperones to neuronal intranuclear inclusions. *Ann. Neurol.*, **51**, 302–310.
36. Takahashi, J., Fujigasaki, H., Zander, C., El Hachimi, K.H., Stevanin, G., Durr, A., Lebre, A.S., Yvert, G., Trottier, Y., The, H. *et al.* (2002) Two populations of neuronal intranuclear inclusions in SCA7 differ in size and promyelocytic leukaemia protein content. *Brain*, **125**, 1534–1543.
37. Calado, A., Tome, F.M., Brais, B., Rouleau, G.A., Kuhn, U., Wahle, E. and Carmo-Fonseca, M. (2000) Nuclear inclusions in oculopharyngeal muscular dystrophy consist of poly(A) binding protein 2 aggregates which sequester poly(A) RNA. *Hum. Mol. Genet.*, **9**, 2321–2328.
38. Perutz, M.F. (1999) Glutamine repeats and neurodegenerative diseases: molecular aspects. *Trends Biochem. Sci.*, **24**, 58–63.
39. Saudou, F., Finkbeiner, S., Devys, D. and Greenberg, M.E. (1998) Huntingtin acts in the nucleus to induce apoptosis but death does not correlate with the formation of intranuclear inclusions. *Cell*, **95**, 55–66.
40. Bence, N.F., Sampat, R.M. and Kopito, R.R. (2001) Impairment of the ubiquitin-proteasome system by protein aggregation. *Science*, **292**, 1552–1555.
41. Jana, N.R., Zemskov, E.A., Wang, G. and Nukina, N. (2001) Altered proteasomal function due to the expression of polyglutamine-expanded truncated N-terminal huntingtin induces apoptosis by caspase activation through mitochondrial cytochrome c release. *Hum. Mol. Genet.*, **10**, 1049–1059.
42. Rosser, T.C., Johnson, T.R. and Warren, S.T. (2002) A cerebellar FMR1 riboCGG binding protein. *Am. J. Hum. Genet.*, **71**, 507.
43. Liquori, C.L., Ricker, K., Moseley, M.L., Jacobsen, J.F., Kress, W., Naylor, S.L., Day, J.W. and Ranum, L.P. (2001) Myotonic dystrophy type 2 caused by a CCTG expansion in intron 1 of ZNF9. *Science*, **293**, 864–867.
44. Savkur, R.S., Philips, A.V. and Cooper, T.A. (2001) Aberrant regulation of insulin receptor alternative splicing is associated with insulin resistance in myotonic dystrophy. *Nat. Genet.*, **29**, 40–47.
45. Van der Werf, Y.D., Witter, M.P. and Groenewegen, H.J. (2002) The intralaminar and midline nuclei of the thalamus. Anatomical and functional evidence for participation in processes of arousal and awareness. *Brain Res. Brain Res. Rev.*, **39**, 107–140.
46. Kilpatrick, I.C., Jones, M.W., Johnson, B.J., Cornwall, J. and Phillipson, O.T. (1986) Thalamic control of dopaminergic functions in the caudate-putamen of the rat—II. Studies using ibotenic acid injection of the parafascicular-intralaminar nuclei. *Neuroscience*, **19**, 979–990.
47. Tanaka, Y., Miyazawa, Y., Akaoka, F. and Yamada, T. (1997) Amnesia following damage to the mammillary bodies. *Neurology*, **48**, 160–165.
48. Sziklas, V. and Petrides, M. (1993) Memory impairments following lesions to the mammillary region of the rat. *Eur. J. Neurosci.*, **5**, 525–540.
49. Oliver, D.L. and Huerta, M.F. (1992) Inferior and superior colliculi. In Webster, D.B., Popper, A.N. and Fay, R.R. (eds), *The Mammalian Auditory Pathway: Neuroanatomy.* Springer, New York, pp. 168–221.
50. Dombrowski, C., Levesque, S., Morel, M.L., Rouillard, P., Morgan, K. and Rousseau, F. (2002) Premutation and intermediate-size FMR1 alleles in 10 572 males from the general population: loss of an AGG interruption is a late event in the generation of fragile X syndrome alleles. *Hum. Mol. Genet.*, **11**, 371–378.
51. Devys, D., Lutz, Y., Rouyer, N., Bellocq, J.P. and Mandel, J.L. (1993) The FMR-1 protein is cytoplasmic, most abundant in neurons and appears normal in carriers of a fragile X premutation. *Nat. Genet.*, **4**, 335–340.
52. Khandjian, E.W., Bardoni, B., Corbin, F., Sittler, A., Giroux, S., Heitz, D., Tremblay, S., Pinset, C., Montarras, D., Rousseau, F. *et al.* (1998) Novel isoforms of the fragile X related protein FXR1P are expressed during myogenesis. *Hum. Mol. Genet.*, **7**, 2121–2128.
53. Tamanini, F., Willemsen, R., van Unen, L., Bontekoe, C., Galjaard, H., Oostra, B.A. and Hoogeveen, A.T. (1997) Differential expression of FMR1, FXR1 and FXR2 proteins in human brain and testis. *Hum. Mol. Genet.*, **6**, 1315–1322.
54. Shibatani, T. and Ward, W.F. (1995) Sodium dodecyl sulfate (SDS) activation of the 20S proteasome in rat liver. *Arch. Biochem. Biophys.*, **321**, 160–166.
55. Bakker, C.E., de Diego Otero, Y., Bontekoe, C., Raghoe, P., Luteijn, T., Hoogeveen, A.T., Oostra, B.A. and Willemsen, R. (2000) Immunocytochemical and biochemical characterization of FMRP, FXR1P, and FXR2P in the mouse. *Exp. Cell. Res.*, **258**, 162–170.
56. Paxinos, G. and Franklin, B.J. (2001) *The Mouse Brain in Stereotaxic Coordinates.* Academic Press, Montreal.